energies

MDPI

Article

Numerical Simulation of Vapor Dropwise Condensation Process and Droplet Growth Mode

Yali Guo, Run Wang, Denghui Zhao, Luyuan Gong * and Shengqiang Shen

National Joint Engineering Research Center for Thermal Energy Integration, School of Energy and Power Engineering, Dalian University of Technology, Dalian 116024, China
* Correspondence: lygong@dlut.edu.cn

Abstract: Compared with film condensation, dropwise condensation based on droplet growth can significantly improve the condensing equipment's water collection and thermal efficiency in the vapor condensate system. Therefore, as a critical behavior affecting the evolution of dropwise condensation, research on droplet growth is of great significance to further understanding the evolutionary characteristics and heat transfer mechanism of dropwise condensation. In this paper, a model for simulating the entire evolution process of dropwise condensation is improved and constructed, and the evolution process of dropwise condensation with different condensation nucleus densities on the vertical wall is simulated based on certain assumptions. Moreover, parameters such as evolution rate and size contribution are proposed to measure droplet growth's influence on the evolution process of dropwise condensation. In the simulation, the Cassie model was used to describe the condensation growth of droplets. The neighbor finding algorithm and conservation law are coupled to simulate the coalescence growth process of droplets. Through the comparison of the theoretical model and experimental results, it is indicated that the simulation method in this paper is highly reliable. The simulation results demonstrate that more than 95% of the maximum droplet size of dropwise condensation is derived from coalescence growth, and its growth rate can characterize the evolution rate of dropwise condensation. The evolution rate reveals a linear growth trend with the increase of condensate nucleus density, and the average heat flux shows an increasing trend followed by a decreasing trend, reaching the peak, $q_{average}$ = 30.5 kW·m^{-2}, at the $N_S = 5 \times 10^9$ m^{-2}. The surfaces with a high coalescence frequency can increase the contribution of the coalescence growth to the maximum droplet size more effectively and, conversely, the contribution of condensation growth is weakened, which is less than 1% at the $N_S = 7.5 \times 10^9$ m^{-2}.

Keywords: dropwise condensation; evolution rate; growth mode; size contribution; contribution proportion

check for updates

Citation: Guo, Y.; Wang, R.; Zhao, D.; Gong, L.; Shen, S. Numerical Simulation of Vapor Dropwise Condensation Process and Droplet Growth Mode. *Energies* **2023**, *16*, 2442. https://doi.org/10.3390/en16052442

Academic Editor: Gabriela Huminic

Received: 29 January 2023
Revised: 22 February 2023
Accepted: 1 March 2023
Published: 3 March 2023

Copyright: © 2023 by the authors. Licensee MDPI, Basel, Switzerland. This article is an open access article distributed under the terms and conditions of the Creative Commons Attribution (CC BY) license (https://creativecommons.org/licenses/by/4.0/).

1. Introduction

Condensation, a typical change in the phenomenon of heat transfer, can be divided into filmwise condensation (FWC) and dropwise condensation (DWC) from the macroscopic view [1]. Generally, the heat transfer coefficient of dropwise condensation is one or several orders of magnitude higher than that of filmwise condensation [2,3]. Therefore, as an efficient method of condensation heat transfer, dropwise condensation has broad application prospects in petrochemical systems, seawater desalination systems, and thermal management systems [4–7]. Generally, dropwise condensation is a physical evolution process of droplet swarm across time and space, involving nucleation, growth, and departure of droplets. The effect of droplet growth on the evolution process is a key problem in the study of the evolutionary characteristics and heat transfer mechanism of dropwise condensation. In accordance with the droplet growth mode, droplet growth can be divided into condensation growth and coalescence growth. The two types of droplet growth occur simultaneously and interact with each other during the evolution process of dropwise

condensation. Consequently, it is of great significance to select appropriate parameters to measure the condensation evolution process and quantitatively analyze the influence of different growth modes on condensation evolution to shorten the departure cycle and enhance the heat transfer capacity.

Since Schmidt et al. [8] reported dropwise condensation in 1930, many scholars have been attracted by this efficient heat transfer method, which is a common phenomenon in life. Scholars have conducted more intensive and extensive research on dropwise condensation through theoretical and experimental methods, which discussed various characteristics of condensation evolution and droplet growth. Graham et al. [9] experimentally studied dropwise condensation heat transfer process and found that 90% of heat transfer is completed by droplets with a diameter of less than 10 μm. It is also pointed out that reducing the droplet departure radius can enhance condensation heat transfer. The experiments of Gose [10] and Rose [11] demonstrated that droplet growth is mainly realized by condensation growth at the initial stage and then coalescence growth when it reaches the critical radius r_c. Later, Tanasawa et al. [12] also found that droplet growth is mainly controlled by the coalescence of neighboring droplets and proposed the equation for the coalescence growth rate of droplets by deduction. Chen et al. [13] compared the average heat flux of droplets of different sizes and concluded that the critical radius ranges are between 0.01 to 0.1 mm, which is consistent with Rose's conclusion. Peng et al. [14] conducted condensation heat transfer experiments on superhydrophobic-hydrophilic surfaces and pointed out that the maximum radius of droplets in the hydrophobic region increased with the increase of the width of the hydrophobic region. Chen et al. [15] observed the evolution process of dropwise condensation in hydrophobic and hydrophilic copper-based microchannels, finding there was a smaller droplet departure radius and shorter cleaning period at high vapor flow rates, resulting in a higher heat transfer coefficient. Alwazzan et al. [16] coated the superhydrophobic coating on the surface of the whole condenser and discovered that the heat transfer effect of condensate water could be improved by increasing the removal rate of condensate water. Bhattarai et al. [17] noticed that when the droplet grew to a certain size, the droplet detached from the surface due to the gravity action. At this point, the larger the contact angle of the droplet, the smaller the departure radius of the droplet, and the shorter the condensation period. Ashrafi-Habibabadi et al. [18] first studied the whole evolution process of dropwise condensation on hydrophobic and superhydrophobic surfaces with different structures. The dynamic changes of condensed droplets were clearly observed, which is of certain significance for realizing surface self-cleaning. Aili et al. [19] analyzed the influence of the wettability and shape of the nucleation position on the nanocones' surface on the droplet growth through experimental observation, indicating that the groove in the medium closed cavity is beneficial to the droplet growth, owing to the weakening of its energy barrier.

Compared to experimental research, the theoretical research of dropwise condensation has also developed rapidly. As early as 1966, Lefevre et al. [20] described dropwise condensation heat transfer model by introducing the heat transfer model of a single droplet and the size distribution function of small-sized droplets. Later, Maa et al. [21] added the size distribution function of large droplets to the model, but the above models only considered the thermal resistance of droplets. Considering the relationship between superhydrophobic surfaces and dropwise condensation, Miljkovic et al. [22] extended the condensation heat transfer model by combining the geometric characteristics of superhydrophobic micro-structured and nano-structured surfaces and researched the effects of surface geometry and coating thickness on the evolution of dropwise condensation. Liu et al. [23] obtained the critical nucleation radius and nucleation density of droplets through thermodynamic analysis by considering four thermal resistances, such as gas–liquid interface thermal resistance, and finally modified the existing dropwise condensation heat transfer model. Han et al. [24] proposed a heat and mass balance coupling model of droplet growth in condensation flow of non-equilibrium uniform wet vapor, which accurately described the droplet growth process in any range of Knudsen number. Shang et al. [25] combined the composite wetting

characteristics with the hierarchical morphology to construct the surface, impelling the droplets rapidly to nucleate and drop, and developed a comprehensive model to further explore this process. Xie et al. [26] derived the density distribution of small-sized droplets in the range of $r_{min} < r < r_c$ and pointed out that reducing the droplet departure radius r_{max} is an important way to enhance the condensation heat transfer on the surface.

With the development of theoretical models and computational science, numerical simulation has been increasingly applied to the research of dropwise condensation. Earlier, Burnside et al. [27] performed numerical simulations of droplets' condensation and coalescence growth process on a 240 μm × 240 μm condensation surface for approximately 0.21 ms. The experiment showed that the maximum droplet size by coalescence growth was several times larger than that of condensation growth. Liu et al. [28] improved the Double Distribution Function (DDF) and simulated the dropwise condensation process of vapor using the Lattice Boltzmann Method on a vertical hydrophobic horizontal plate. It was noted that the condensation time of the droplets decreased with the increase of the surface contact angle. Pawar et al. [29] also used the lattice Boltzmann method to study the relationship between nucleation time and surface wettability. This investigation has indicated that, the better the surface wettability, the shorter the nucleation time, and the easier the formation of condensed droplets. Bahrami et al. [30] simulated dropwise condensation in micro-structured and nano-structured inclined tubes by adopting a suitable numerical model. The results showed that the vertical tube has a good mass transfer rate. Zhao et al. [31] analyzed the droplet size distribution under different condensation nucleus densities based on the model of the whole evolution process of dropwise condensation and found that the density of small-sized droplets increased with the improvement of condensation nucleus density on the condensation surface. Based on the dynamic numerical simulation method, Azarifar et al. [32] combined the Marangoni convection and interface mass transfer with surface tension to simulate the condensation growth of droplets. The results highlight the importance of heat transfer of small-sized droplets where convection is not dominant.

In recent years, many scholars have begun to employ Molecular Dynamics (MD) as a new tool to simulate condensation phenomena and explore the growth characteristics and heat and mass transfer of droplets or liquid films [33–39]. For example, Sun et al. [33] studied the initial and middle stages of vapor condensation on smooth surfaces based on the MD method. The results indicated that the relative magnitude of the interface resistance and the thermal resistance of condensed droplet were related to time. The former plays a major role in the initial stage of condensation, and the latter gradually dominates over time. Niu et al. [34] obtained the relationship between solid–liquid interface thermal resistance and solid surface wettability during the process of droplet nucleation based on the MD simulation method. The results demonstrated that the critical nucleation radius increases significantly after the addition of solid-liquid interface thermal resistance, while the nucleation density decreases. Ghahremanian et al. [36] investigated the effect of nanoparticles on the annular condensation flow of argon-copper nanofluids in nanochannels by the MD method. It is observed that the addition of nanoparticles destroys the density distribution and brings the liquid film closer to the wall and center of the nanochannel.

In summary, most of the studies on droplet growth characteristics are focused on the viewpoint of single droplet heat transfer, which is limited to a certain condensation stage, while ignoring the macroscopic influence of droplet growth behavior on the dropwise condensation evolution process, lacking quantitative analysis of the contribution of different growth modes to droplet growth and the evolution process. Furthermore, the existing research pays insufficient attention to the evolution rate of dropwise condensation, and the departure radius cannot accurately describe the rate of condensation evolution. In order to deeply understand the influence of droplet growth behavior on the condensation evolution process, based on numerical simulation, this paper studies the entire evolution process of dropwise condensation with variable condensation nucleus density on the vertical wall. Compared with previous simulation studies, the algorithm of neighbor finding is used to collect adjacent droplets, and

the finding process is accelerated by limiting the search range. In addition, this paper also improves the departure model of droplets to update their spatial position and velocity. The droplet renucleation model is refined and the judgment conditions of regional renucleation are considered. Condensation growth and coalescence growth behavior of droplets were integrated into the droplet growth model. Additionally, the concepts of evolution rate and size contribution are proposed to study droplet growth characteristics.

Therefore, from the perspective of condensation evolution, based on the initial nucleation, growth, departure, and renucleation of droplets, a model of the entire evolution process of dropwise condensation was established in this paper. In the simulation, the Cassie model was used to describe the condensation growth of droplets. The algorithm of neighbor finding and conservation law are coupled to simulate the coalescence growth process of droplets. Numerical simulation was carried out on a 0.004 m × 0.004 m vertical hydrophobic surface to study the evolution process of dropwise condensation. The effect of different growth modes on the evolution of dropwise condensation is investigated by changing the initial condensation nuclei on the hydrophobic surface. The simulation results showed the evolution process of dropwise condensation on the vertical hydrophobic, reproducing the behaviors of droplets' nucleation, growth, and coalescence, revealing the influence of condensation nucleus density and growth mode on dropwise condensation evolution and the heat transfer effect. The experimental results and the theoretical model demonstrated that the simulation method was highly feasible and reliable.

2. Method

2.1. Model of the Whole Evolution Process of Dropwise Condensation

Dropwise condensation is a physical evolution process of droplet swarms across time and space, including the initial nucleation, renucleation, growth, and departure of droplets. In terms of the evolution process, independent droplet behavior occurring continuously and reciprocally during the condensation process provides a source of power for the evolution of dropwise condensation and impels the condensation heat transfer to evolve towards a steady state. Therefore, based on different droplet behaviors of vapor dropwise condensation, the model of the whole evolution process of dropwise condensation in this paper was divided into three parts: the droplet nucleation model, the droplet growth model, and the droplet departure model.

2.1.1. Droplet Nucleation and Renucleation

The droplet nucleation in the evolution of dropwise condensation includes the initial nucleation process and the renucleation process. This paper simulated the droplet nucleation behavior based on the fixed nucleation center hypothesis [40]. In the simulation, the condensation nucleus densities N_S ranges from 10^9 to 10^{10} m^{-2}, and all condensation nuclei in the computational domain have the same fixed initial nucleation radius, which is given by [41]:

$$r_{min} = \frac{2T_{sat}\sigma}{H_{fg}\rho\Delta T} \quad (1)$$

where, T_{sat} is vapor saturation temperature, σ is the surface tension coefficient, H_{fg} is the internal latent heat of condensate water, ρ is the density of condensate water, and ΔT is the surface subcooling.

At the very beginning of the evolution process of dropwise condensation, the condensation nuclei demonstrate uniformly random distribution [31]. Subsequently, the renucleation droplets' position remained unchanged. The computational domain was divided into a square net according to the spacing of $l = 1/\sqrt{N_S}$ and the mean spacing of the condensation nuclei was $l/2$. The distribution of condensation nuclei is shown in Figure 1.

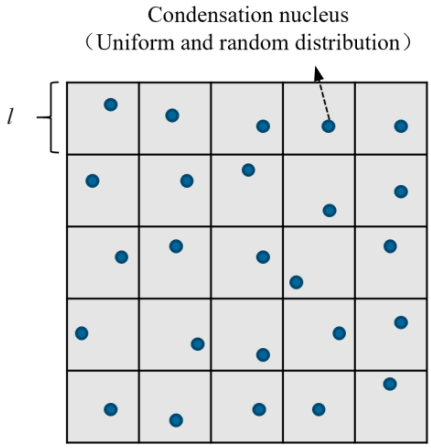

Figure 1. Distribution of condensation nuclei.

For renucleation, the nucleation takes place at the surface region that is uncovered by the grown droplets. During the process of condensation, the size and position of the droplet changed with time due to its growth and departure. The droplet no longer nucleated at fixed nucleation sites already covered by other droplets. Therefore, whether the original fixed nucleation site will nucleate again needs to be re-evaluated, and the renucleation needs to meet the following condition:

$$\sqrt{(x_{\min} - x_{\text{side}})^2 + (y_{\min} - y_{\text{side}})^2 + (z_{\min} - z_{\text{side}})^2} \leq r_{\min} + r_{\text{side}} \tag{2}$$

where $(x_{\min}, y_{\min}, z_{\min})$ represents the spatial position of the condensation nuclei, $(x_{\text{side}}, y_{\text{side}}, z_{\text{side}})$ represents the spatial position of the nearest droplet to this nucleus, and $r_{\min}$ and r_{side} are the radii of the above nuclei and droplet respectively.

2.1.2. Droplet Growth

The mode of droplet growth in the evolution process of dropwise condensation can be divided into condensation growth and coalescence growth. The droplet growth behavior is simulated in this paper based on two such growth modes.

In the case of condensation growth, water vapor condenses directly on the droplet surface, contributing to the growth of the droplets. The condensation growth behavior of the droplet continues in the cross-scale evolution process of dropwise condensation. For the condensation growth of a single droplet, the expression for the dropwise condensation growth rate G is found to be [42,43]:

$$G = \frac{\mathrm{d}r}{\mathrm{d}t} = \frac{q_{\mathrm{d}}}{\rho H_{\mathrm{fg}} 2\pi r^2 (1 - \cos\theta)} \tag{3}$$

where q_{d} is the droplet heat transfer rate, r represents the droplet radius, and θ means the contact angle of droplets. The simulation used the thermal resistance model based on the Cassie growth model of dropwise condensation [22,43,44], as shown in Figure 2.

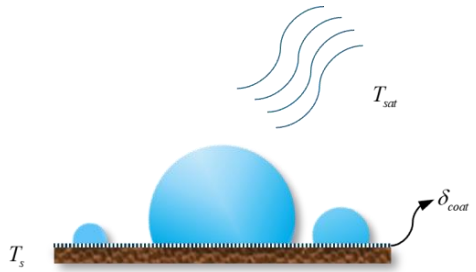

Figure 2. Thermal resistance model of droplet condensation growth.

The expression of heat transfer rate for a single droplet q_{d} is defined as [43]:

$$q_{\mathrm{d}} = \frac{\Delta T \pi r^2 (1 - r_{\min}/r)}{\left(\frac{\delta}{k_\delta \sin^2\theta} + \frac{r\theta}{4k_{\mathrm{w}} \sin\theta} + \frac{1}{2h_{\mathrm{i}}(1-\cos\theta)}\right)} \tag{4}$$

where δ is the thickness of the hydrophobic coating, k_δ means the coefficient of heat conduction of hydrophobic film, k_{w} indicates the coefficient of heat conduction of water, and h_{i} represents the heat transfer coefficient of the gas-liquid section. Substituting Equation (4) into Equation (3), the single dropwise condensation growth rate G can be reduced:

$$G = \frac{\Delta T}{2\rho H_{\mathrm{fg}}} \frac{1 - r_{\min}/r}{\frac{r\theta(1-\cos\theta)}{4k_{\mathrm{w}} \sin\theta} + \frac{\delta(1-\cos\theta)}{k_\delta \sin^2\theta} + \frac{1}{2h_{\mathrm{i}}}} \tag{5}$$

It can be seen from Equation (5) that the condensation growth rate of a single droplet only changes with the variation of the radius of the droplet under the same condensation thermal parameters and condensing surface properties. As the droplet radius increases, the single droplet condensation growth rate shows an increasing trend followed by a decreasing trend, which is consistent with the dropwise condensation growth observed in the experiment [45].

When the droplet shape is an ideal spherical crown, the dropwise condensation growth at a given step size Δt can be described by the following equation for the droplet radius r:

$$r_n = r_b + \Delta r_l \tag{6}$$

where r_b and r_n are the radii of the droplet before and after the condensation growth within time Δt and Δr_l is the radius increase (or size contribution) of the droplet in the dropwise condensation growth behavior within Δt.

For the coalescence growth of two droplets, the droplet is inclined to coalesce with the nearest droplet, resulting in an increase in size and change in location. In contrast to condensation growth, droplet coalescence growth shows clearly discontinuous characteristics in the cross-scale evolution process of dropwise condensation, and its occurrence requires meeting specific droplet coalescence conditions. As shown in Figure 3, the coalescence condition for two adjacent droplets (i and j) in the simulation is:

$$l_{ij} \le r_i + r_j \tag{7}$$

where l_{ij} is the actual distance between two adjacent droplets and r_i and r_j are their radii. The sum of r_i and r_j is the theoretical limit of the contact distance between the two droplets on a vertical hydrophobic surface. l_{ij} is calculated as:

$$l_{ij} = \left((x_i - x_j)^2 + (y_i - y_j)^2 + (z_i - z_j)\right)^{1/2} \tag{8}$$

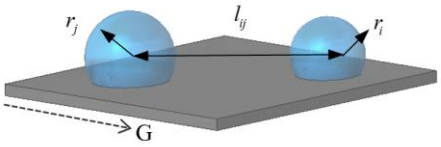

Figure 3. Schematic diagram of droplet coalescence judgment.

In the above equation, the spatial position of the droplet is described by Cartesian coordinates (x,y,z), where the x and y axes represent the width and height directions of the vertical wall, respectively, and the z axis represents the direction perpendicular to the wall. The y coordinate of the droplet is constantly updating due to the coalescence growth or departure of the droplet, whereas the x coordinate of the droplet is only influenced by

the coalescence growth. As for the z coordinate, when the droplet is considered an ideal spherical crown, it can be deduced by $z = r\cos(\pi - \theta)$ and the calculation is affected by the droplet growth.

When two adjacent droplets meet the coalescence condition, the two droplets coalesce into a new droplet, achieving coalescence growth compared to the two original droplets. The size, spatial position, and motion state of the new droplet are determined by the state of the two original droplets. Firstly, the size of the new droplet, r_{new}, can be obtained using the following equation [41]:

$$r_{new} = \left[\frac{3V_{new}}{\pi(2 - 3\cos\theta + \cos^3\theta)}\right]^{1/3} \tag{9}$$

If the maximum size of two adjacent droplets is $r_{\max(i,j)}$, then $\Delta r_h = r_{new} - r_{\max(i,j)}$ is defined as the contributor to the growth behavior to the droplet.

Moreover, based on the conservation law of mass, the volume of the new droplet is written as $V_{new} = V_i + V_j$, where V_i and V_j are the volumes of the two adjacent droplets before coalescence. Secondly, the spatial position of the new droplet (x_{new},y_{new},z_{new}) can be obtained from the conservation law of nature's heart, which is given by:

$$\begin{cases} x_{new} = \left(\rho V_i x_i + \rho V_j x_j\right)/\rho V_{new} = \left(V_i x_i + V_j x_j\right)/V_{new} \\ y_{new} = \left(\rho V_i y_i + \rho V_j y_j\right)/\rho V_{new} = \left(V_i y_i + V_j y_j\right)/V_{new} \\ z_{new} = r_{new}(\pi - \cos\theta) \end{cases} \tag{10}$$

In addition, the droplet's state of self-motion can be updated according to the conservation law of momentum. In the evolution process of dropwise condensation, the droplet only has two motion states: standstill and departure. When there is a departing droplet (i or j) in the coalescence, the departure velocity v_{new} of the new droplet can be expressed as:

$$v_{new} = \left(\rho V_i v_i + \rho V_j v_i\right)/\rho V_{new} = \left(V_i v_i + V_j v_j\right)/V_{new} \tag{11}$$

When the original droplets are all at rest, the motion state of the new droplet after the coalescence growth needs to be re-evaluated. The discrimination method can be seen in the following section.

2.1.3. Droplet Departure

Droplet departure on a vertical hydrophobic surface can occur in two ways: gravity-driven droplet departure and surface energy release-led droplet bouncing. The latter has a higher demand on the surface property of the material and rarely lasts over time under the research conditions of this paper. In contrast, gravity-driven droplet departure is the dominant mode of detachment from vertical hydrophobic surfaces. Therefore, in this paper, only gravity-led droplet departure is considered. As shown in Figure 4, the droplet departure behavior of dropwise condensation on a vertical hydrophobic surface refers to the departure of large droplets subject to both droplet capillary forces and gravity.

The droplet departure behavior occurs at the later stage of the evolution process of dropwise condensation, and the droplet departure is discerned by:

$$F_g > F_c \tag{12}$$

where F_g and F_c are the gravity and capillary forces on the vertical hydrophobic surface of the droplet. If the former is greater than the latter, the droplet starts to depart. The above two forces are calculated as follows [43]:

$$\begin{cases} F_g = \frac{2-3\cos\theta+\cos^3\theta}{3}\pi r^3\rho g \\ F_c = 2cr\sin\theta\sigma(\cos\theta_r - \cos\theta_a) \end{cases} \tag{13}$$

where g is the acceleration of gravity, c is the capillary force constant, c usually equals 1, θ_r represents the droplet regression angle, and θ_a indicates the droplet advance angle. The above formula shows that, when the condensing surface properties are stable and the droplet contact angle remains unchanged, the droplet gravity and capillary forces are only a function of the radius r. Droplet gravity presents exponential growth, while capillary force presents linear growth with the variance of droplet radius. This means that the droplet capillary force increases faster than the gravitational force and, as the dropwise condensation process evolves to a certain stage, the large droplets will depart.

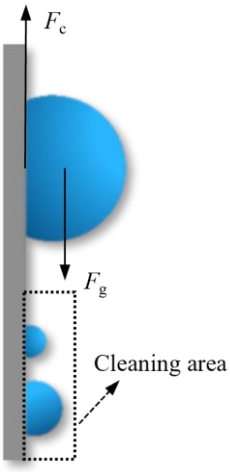

Figure 4. Schematic diagram of droplet departure.

When the droplet radius meets the departure condition, the droplet starts to depart and slide. The distance $S_{\Delta t}$ the droplet slides within Δt is:

$$S_{\Delta t} = v_b \Delta t + \frac{1}{2} a (\Delta t)^2 \tag{14}$$

where v_b is the initial velocity of the departed droplet, which equals zero when the droplet is at a resting state. The droplet detachment velocity v_n after Δt can be obtained according to $v_n = v_b + a\Delta t$. It is clear that, when Δt is taken to be small enough, the droplet motion within the Δt can be considered in uniform acceleration motion. Hence, the acceleration of the departure droplet within the Δt can be regarded as a constant and a is taken to be the average acceleration of the droplet within Δt.

The spatial position (y_n) of the droplet can be updated according to the distance $S_{\Delta t}$ the droplet slides in Δt. It can be expressed by:

$$y_n = y_b - S_{\Delta t} \tag{15}$$

where y_b and y_n are the y coordinates of the droplet before and after Δt, respectively.

If the droplet does not satisfy the departure condition, no departure will occur. Then the droplet's departure velocity equals zero. In the meantime, if the coalescence condition is also not met, the droplet's spatial position remains unchanged.

2.2. Simulation Method

2.2.1. Simulation Procedure and Algorithm

To sum up, based on the model of the whole evolution process of dropwise condensation, this paper further improves the numerical simulation method [20–26] to simulate the evolution processes of dropwise condensation on the vertical hydrophobic surface. The updated simulation method is based on the following assumptions:

1. The formation position of condensation nuclei is fixed, and the condensation nuclei demonstrate uniformly random distribution;

2. The droplet is considered an ideal spherical crown when computing its spatial position and size;
3. The process of droplet coalescence growth will complete instantaneously regardless of the coalescence time [25,46];
4. The property of the hydrophobic surface is uniform, and the droplets have the same contact angle.

In the simulation process, the condensation conditions and surface properties were the first set-up. After the initial nucleation of droplets, the whole evolution process of dropwise condensation was discretized. All droplets in each time step were judged and examined for renucleation, growth, and departure so as to update their size, spatial position, and the motion state of the droplet swarms on the vertical hydrophobic surface at a specific time. Such a simulation process was iterated until a large droplet departed from the vertical hydrophobic surface. The flow chart of the simulation method is shown in Figure 5.

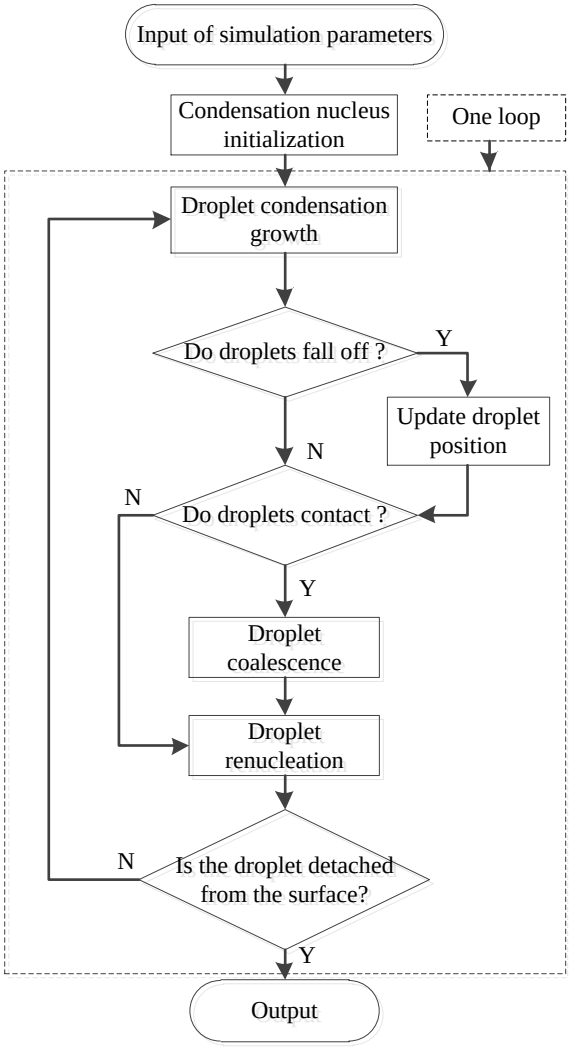

Figure 5. Flow chart of the simulation procedure.

In the simulation, for the coalescence growth of a droplet (x_i,y_i,z_i,r_i), the algorithm of neighbor finding was used to search for the coalescence droplets (x_j,y_j,z_j,r_j) and to speed up the search process by defining the search area. The search area for a coalescence droplet can be defined as:

$$\begin{cases} x_i - 2r_i \le x_j \le x_i + 2r \\ y_i - 2r_i \le y_j \le y_i + 2r \end{cases} \quad (16)$$

The coalescence droplets searched by the algorithm of neighbor finding may not be unique, but are all involved in the coalescence growth of the droplet. Alternatively, the algorithm of neighbor finding can be used to determine the renucleation on the hydrophobic surface and find the nearest droplet to a fixed nucleation site. The renucleation condition of the fixed formation position is introduced in Section 2.1.1.

When departure occurs, the departing droplets will make a wiping action to all the droplets that are on the departure route. In the simulation, the process of the wiping route of the departing droplets is described according to the coalescence growth mode of the droplets.

2.2.2. Simulation Parameters

The computational domain for the numerical simulation of the evolution process of dropwise condensation is a vertical hydrophobic surface of 0.004 m long and 0.004 m wide. Within this computational domain, dropwise condensation in the range of 10^9 m^{-2}–10^{10} m^{-2} of condensation nucleus densities was simulated in this paper. In the simulation, the droplet's contact angle equals 120°, the advance angle 125°, and the regression angle 115°. The parameter setting of the single droplet thermal resistance model can refer to Equation (4), and the specific condensing condition and surface property parameters are shown in Table 1.

Table 1. Simulation parameters.

Condensation Conditions and Surface Properties	Value
Surface subcooling ΔT/K	1
Saturation temperatures T_{sat}/K	359.08
Surface tension coefficient σ/N·m^{-1}	0.0616
Condensate water density ρ/kg·m^{-3}	968
Latent heat of condensed water H_{fg}/J·kg^{-1}	2.293×10^6
Thickness of hydrophobic coating δ/mm	0.01
Water thermal conductivity k_w/W·m^{-1}·K^{-1}	0.6707
Heat transfer coefficient of gas-liquid section h_i/W·m^{-2}·K^{-1}	106
Thermal conductivity of hydrophobic membrane k_δ/W·m^{-1}·K^{-1}	1000

2.3. Reliability Demonstration of the Simulation

In terms of condensation heat transfer, the evolution process of dropwise condensation can be divided into two stages: dynamic heat transfer and steady heat transfer. In the initial stage of dropwise condensation, the sizes of the droplet swarm are small, and the hydrophobic surface has a high heat transfer capacity. As the evolution continues, the number of larger droplets on the surface gradually increases and the heat transfer effect of condensation decreases dynamically until the droplet size distribution stabilizes, at which point dropwise condensation reaches the steady heat transfer stage.

Based on the two heat transfer stages of the evolution progress described above, the reliability of the numerical simulation method for dropwise condensation was verified in two ways in this paper. As an important parameter for evaluating the steady heat transfer of dropwise condensation, the reliability of the simulation of dropwise condensation in the steady heat transfer state was first verified from the perspective of the droplet size distribution. The density of the condensation nucleus used for the simulation was $N_S = 10^{10}$ m^{-2} and the rest of the condensation conditions and surface properties were listed in Section 2.2.2. The comparison of the droplet size distribution between numerical simulations of dropwise condensation in steady heat transfer and the theoretical model of Rose and Kim [11,43] is shown in Figure 6.

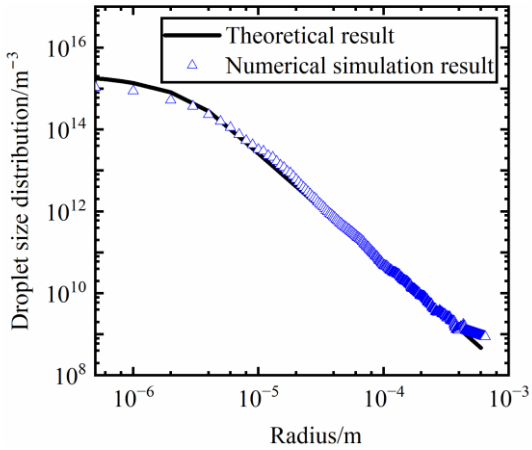

Figure 6. Comparison of droplet size distribution between numerical simulation and theoretical model [11,43].

As can be seen in Figure 6, the droplet size distribution in this simulation is inosculate with the theoretical results of Rose and Kim for the full size of the droplet, thus validating the reliability of the numerical simulation method for modeling dropwise condensation in steady heat transfer.

Additionally, the maximum droplet size and dynamic droplet size distribution, two critical variables in describing the evolution process of dropwise condensation, can be used to verify the reliability of dropwise condensation simulations under dynamic heat transfer conditions. The parameters of the simulation validation are consistent with the experimental parameters of the literature [47]. Under dynamic heat transfer, the comparison of the size range of the maximum droplet between the numerical simulation and the experiment of dropwise condensation is shown in Figure 7.

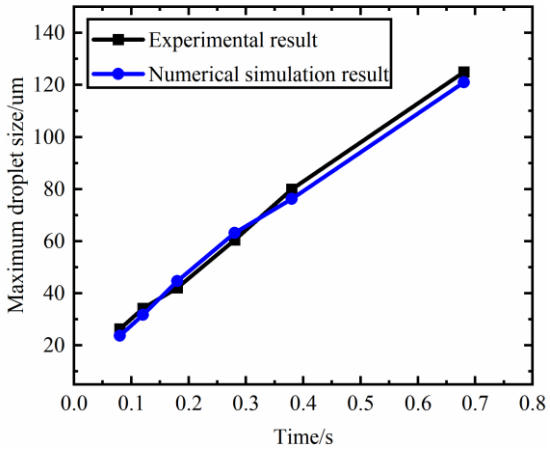

Figure 7. Comparison of maximum droplet size range between numerical simulation and experiment [47].

As can be seen in Figure 7, the simulation results match well with the experimental results for the same evolution time in terms of maximum droplet size. The comparison of droplet size distribution between the numerical simulation and the experiment investigating dropwise condensation under dynamic heat transfer of four moments is shown in Figure 8. The figure illustrates that the simulation results of the droplet size distribution tend to be consistent with the experimental results at the four moments of the evolution process of dropwise condensation, especially those of the large-size droplet data. In addition to this, compared with the experimental study, the simulation can obtain data on the droplet size distribution of smaller drops. The above verifies the reliability of the numerical

simulation method to simulate the evolution process of dropwise condensation under dynamic heat transfer, reflecting the advantages of acquiring data on numerical simulation.

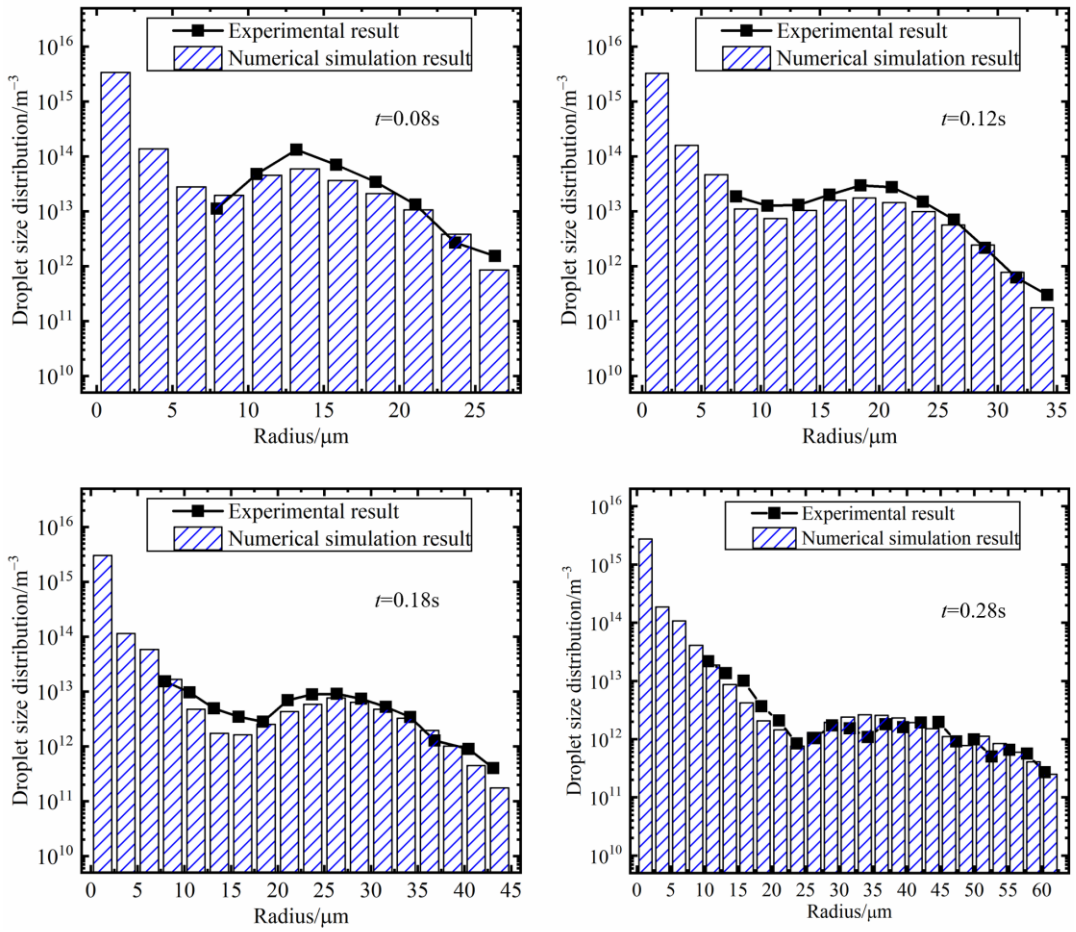

Figure 8. Comparison of droplet size distribution between numerical simulation and experiment [47].

In summary, this paper validates the numerical simulation method for dropwise condensation through the lens of droplet size distribution and maximum droplet size, thus verifying the reliability of the numerical simulation method for modeling the whole evolution process of dropwise condensation and reflecting the advantages of this method.

3. Results and Discussion

3.1. Dropwise Condensation Process

3.1.1. Droplet Growth and Condensation Evolution

As shown in Figure 9, droplet growth modes can be divided into condensation growth and coalescence growth in the evolution process of dropwise condensation. From the perspective of the droplet swarm on the condensing surface, the growth behavior of droplets is continuous and global. In the evolution process, the condensation growth during the condensation growth mode affects all droplets on the hydrophobic surface and continues indefinitely. The rate of the droplet condensation growth is only related to its heat transfer performance. The better the heat transfer performance is, the faster the condensation growth rate. In contrast, for coalescence growth mode, the growth behavior of droplets is discrete and partial. The condensation growth of adjacent droplets is intermittent in the evolution process, and the droplets affected by the growth mode are only confined to the droplets that contact each other on the condensation surface. The condensation growth rate of the droplet is influenced by the relative size of the coalescence droplets. The smaller the relative size gap is, the faster the combined growth rate is. Additionally,

Figure 9 shows the spatial distribution, size change, and behavior characteristics of droplets in the evolution process of dropwise condensation on the vertical hydrophobic surface when the density of the condensation nucleus $N_S = 7.5 \times 10^9$ m^{-2}, where G is the direction of gravity on the droplets. Figure 8 demonstrates that at the initial stage of the evolution process, condensation nuclei and small-sized droplets grow faster due to condensation growth, and the spatial distribution of droplets is relatively uniform at this stage. As the evolution process continued, droplets with relatively larger sizes gradually appeared, and the growth of the largest droplet began to rely on coalescence. When the largest droplet on the surface meets the departure condition, the droplet begins to fall off and complete the surface wiping process. Subsequently, the evolution of the dropwise condensation process develops to the final stage. At this stage, both the droplet size distribution and condensation heat transfer gradually stabilize.

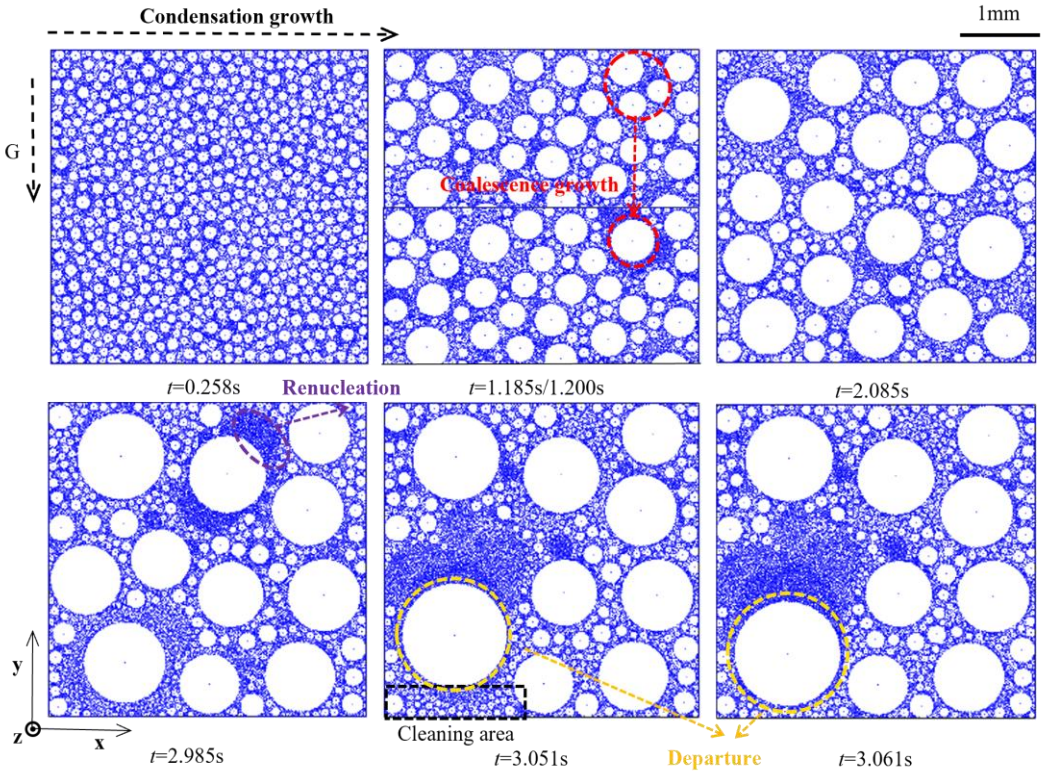

Figure 9. Evolution process of dropwise condensation on the vertical hydrophobic surface.

3.1.2. Characterization of the Evolution Rate of Dropwise Condensation Process

The evolution of dropwise condensation on the vertical hydrophobic surface involves the continuous growth of the droplet swarm until the droplet departure, which is closely related to the variation of droplet size on the surface. Figures 10 and 11 respectively display the comparison between the maximum droplet size change rate and the average droplet size change rate, maximum droplet size, and average droplet size in the above evolution process of droplet condensation. It can be seen from Figures 10a and 11a that the change rate of the maximum droplet size is positive throughout the process of condensation evolution, indicating that the maximum droplet size keeps increasing until the largest droplet falls off the surface. As a comparison, Figure 10b shows the change rate of the average droplet size for all droplets. It shows that the average droplet diameter dramatically drops at the initial stage of the evolution process due to condensation growth and then fluctuates around zero, indicating the average droplet size has reached a stable stage, as shown in Figure 11b.

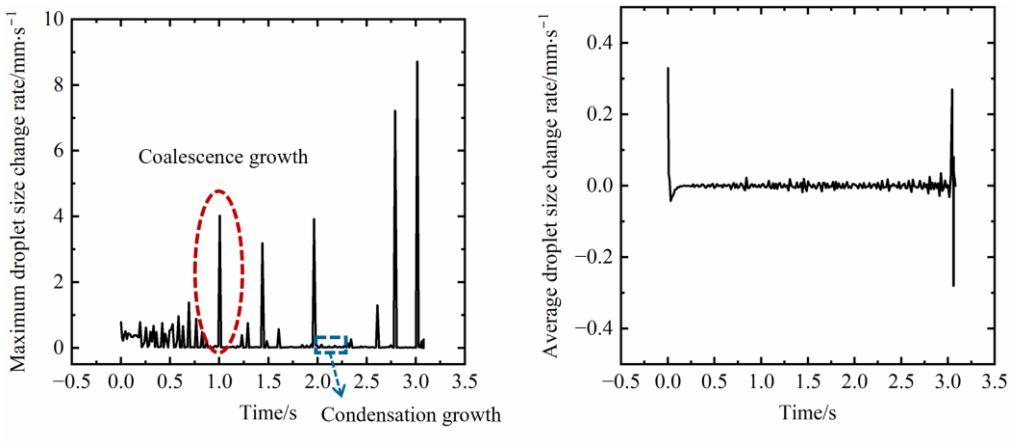

(**a**) (**b**)

Figure 10. Comparison of change rate of maximum droplet size and average droplet size; (**a**) Maximum droplet size change rate and (**b**) Average droplet size change rate.

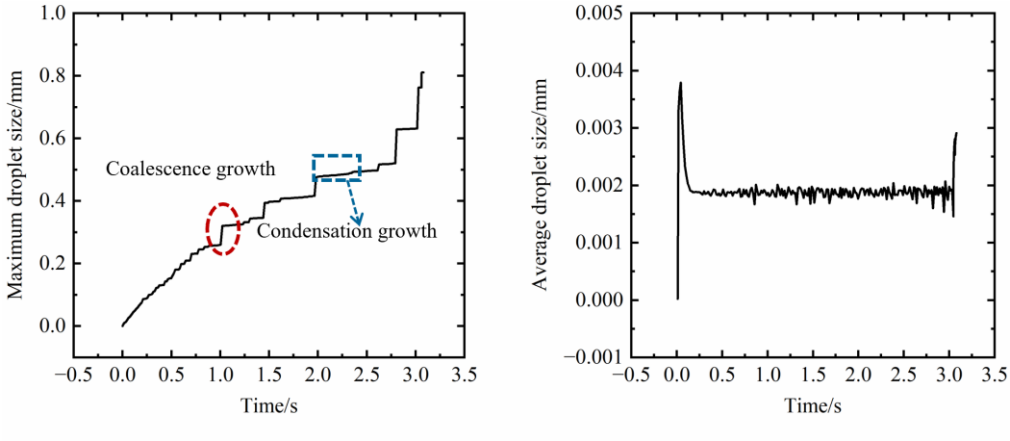

(**a**) (**b**)

Figure 11. Comparison of size of maximum droplet and average droplet; (**a**) Maximum droplet size and (**b**) Average droplet size.

In addition to this, Figure 10 demonstrates that the range of the maximum droplet size change rate is one order larger than the average droplet size change rate. It clearly demonstrates the influence of different growth modes on the evolution process of dropwise condensation. In conclusion, compared with the average droplet size change, the maximum droplet size change can more intuitively reflect the evolution process of dropwise condensation. Therefore, the maximum droplet size change rate is adopted in this paper. It is used to measure the rate of the evolution process of dropwise condensation.

3.2. The influence of Nucleus Densities on the Evolution Rate and Heat Transfer of Dropwise Condensation

3.2.1. The Influence of Nucleus Densities on the Evolution Rate of Dropwise Condensation

As one of the significant property parameters of dropwise condensation surface, the condensation nucleus density has a great effect on the evolution rate of dropwise condensation. The maximum droplet size changes corresponding to different surface condensation nucleus densities are presented in Figure 12. As shown in the chart, with the rise of condensation nucleus density, the growth rate of the maximum droplet size accelerates on the condensation surface. Consequently, the droplets are more likely to reach the theoretical departure radius and fall off in a short time, which is conducive to the improvement of the evolution rate of dropwise condensation, thus prompting the

evolution process. The reason for this phenomenon is that, in the early stage of the dropwise condensation evolution process, the average distance between droplets on the hydrophobic surface with high condensation nucleus density is smaller. As a result, it causes the small-sized droplets to coalesce and grow earlier, and the larger droplets are more likely to appear. Eventually, the coalescence of many large-sized droplets also accelerates the increase of the maximum droplet radius on the surface and eventually advances the evolution process.

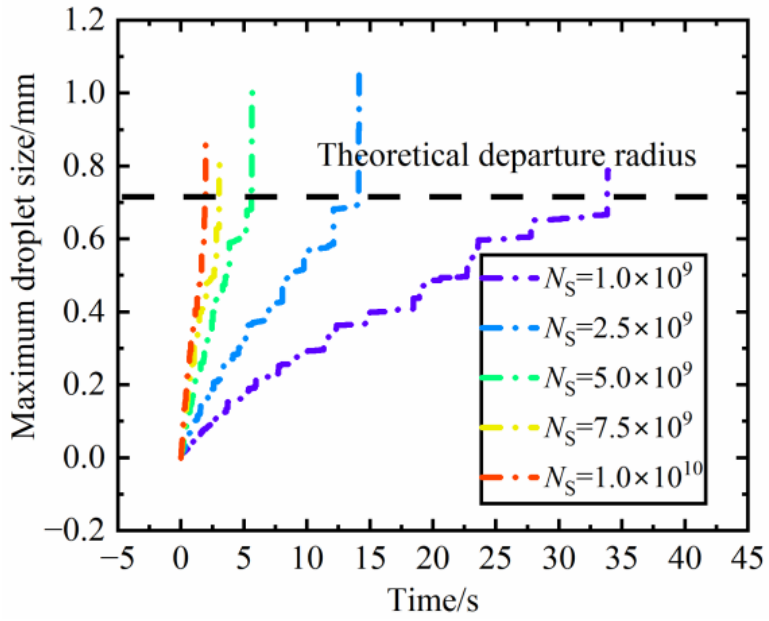

Figure 12. Variation of maximum droplet size under different nucleus densities.

3.2.2. The Influence of Nucleus Densities of Surface Condensation on the Heat Transfer of Dropwise Condensation

Dropwise condensation has diverse heat transfer effects with different surface condensation nucleus densities. Figure 13 demonstrates the relation between maximum droplet size growth rate (v_{rmax}) and average heat flux($q_{average}$) at varying nucleus densities of surface condensation. As can be described from the chart, with the increase of condensation nucleus density, the evolution rate of dropwise condensation represented by the maximum radius growth rate increases linearly. It can advance the shedding time of the largest droplet at high condensation nucleus density, which proves the conclusion above in this paper. Additionally, within a certain range of condensation nucleus densities, the average heat flux first increases and then decreases during the whole evolution process, and the summit, $q_{average}$ = 30.5 kW·m^{-2}, appears around $N_S = 5 \times 10^9$ m^{-2}. It can be concluded that, when the condensation nucleus density is at a low level (before $N_S = 5 \times 10^9$ m^{-2}), its increase can significantly improve the heat transfer capacity of the condensation surface. This is because even smaller droplets are easily formed on the surface of high condensation nucleus density at the initial stage of condensation, which is conducive to heat transfer. At the same time, the improvement of nucleus density accelerates the evolution rate of droplet condensation and promotes the cleaning of departure droplets, and large-sized droplets are not easy to appear. However, the more surface condensation nucleus density speeds up the evolution, the more the heat transfer capacity of dropwise condensation decreases after reaching its peak. The reason for this is that, when the density of the condensation nucleus exceeds a critical value, large-sized droplets are more likely to appear and occupy too much heat transfer surface and condensation time. Apparently, larger-sized droplets are inclined to have less local heat transfer rate due to larger heat transfer resistance.

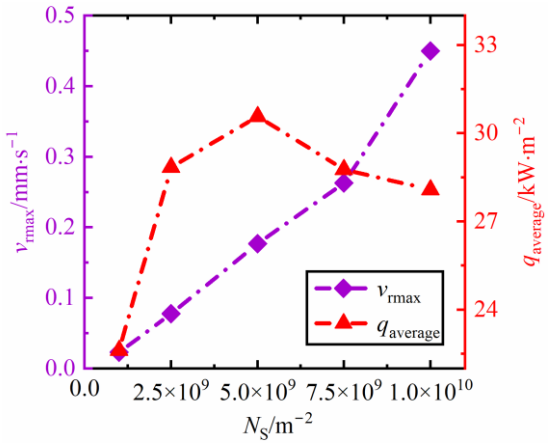

Figure 13. Maximum radius growth rate and average heat flux under different nucleus densities.

3.3. The Influence of Droplet Growth Modes on the Evolution Process of the Dropwise Condensation

3.3.1. The Contribution of Diverse Growth Modes to the Maximum Droplet Size

From the above analysis, it can be seen that the largest droplet size change is the key to studying the evolution process of dropwise condensation. For the largest droplet on the surface, different growth modes contribute differently to the size of the maximum droplet at different evolution stages. Figure 14 shows the comparison of the size contribution of the two growth modes to the maximum droplet size in the evolution process of dropwise condensation with the nucleation density of N_s equal 5×10^9 m^{-2}.

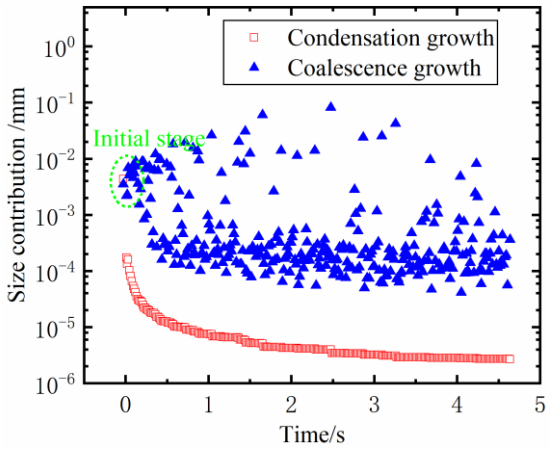

Figure 14. Comparison of the contribution of two growth modes to the maximum droplet size.

It can be seen from the chart that, at the initial stage of dropwise condensation, there is a small discrepancy in contribution between the two growth modes on the maximum droplet diameter. As the evolution process continues, the contribution of condensation growth to the size of the maximum droplet decreases logarithmically, while the coalescence growth fluctuates with time. Although the fluctuation range of the coalescence growth increases first and then decreases, its total contribution to the droplet size is much larger than that of condensation growth. It indicates that the size contribution of condensation growth to the maximum droplet is far greater than that of condensation growth and begins to dominate the growth of the maximum droplet on the surface. Until the later stage of the largest droplet's shedding, the size contribution of the two growth modes to the droplet differs by nearly two orders of magnitude. These results indicate that the coalescence growth mode has a more palpable influence on the evolution of dropwise condensation. Throughout the evolution process of dropwise condensation, the size of the growth of the maximum droplet is mainly the result of coalescence growth (more than 95% of the

maximum droplet size, See Figure 15). Conversely, the impact of the condensation growth is minor and can even be discarded in the later period.

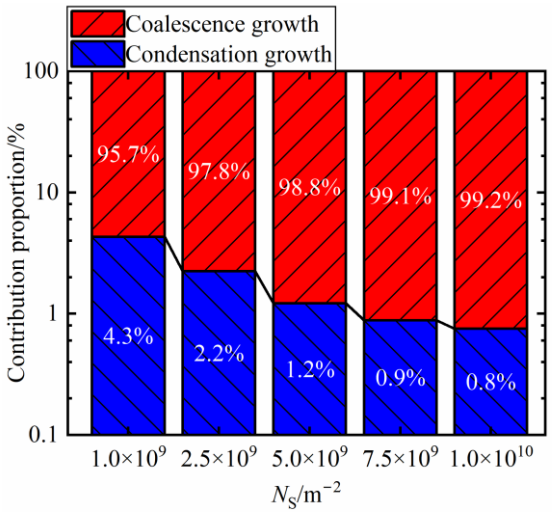

Figure 15. Change of contribution proportion of two growth modes to the maximum droplet size under different nucleus densities.

3.3.2. The Contribution Ratio of two Growth Modes under Different Nucleus Densities

During the evolution of droplet condensation, the contribution of two growth modes to the size of the maximum droplet is also greatly affected by the density of the condensation nucleus. In order to better measure the contribution of varied growth modes to the size of the maximum droplet in the evolution process, a parameter named "contribution proportion" is introduced in this paper:

$$\text{Contribution proportion} = \frac{\text{The size contribution of a growth mode}}{\text{Maximum droplet size}} \quad (17)$$

Figure 15 shows the contribution proportion of the two growth modes to the maximum droplet size at different surface condensation nucleus densities. As can be learned from the figure, with the increment of surface condensation nucleus density, the contribution proportion of condensation growth mode to the size of the maximum droplet continues to decline. Although the decay rate is slowing down, its value is less than 1% when the nucleus density N_S equals 7.5×10^9 m^{-2}. In contrast, the contribution proportion of the coalescence growth mode to the size of the maximum droplet is increasing, which has been maintained at a high level. These results indicate that, with the increase of surface condensation nucleus density, the size increment of the maximum droplet on the surface of dropwise condensation is more dependent on the coalescence growth. At the same time, it is also verified that the faster evolution of dropwise condensation under the higher condensation nuclear density owes to the coalescence growth behavior of the droplet swarm.

3.3.3. The Coalescence Frequency at Different Nucleus Densities

The influence of coalescence growth behavior on the evolution process of dropwise condensation is also reflected in the coalescence frequency of surface droplet swarm. Figure 16 shows that, in the case of high condensation nucleus density, the coalescence frequency of droplet swarm on the condensation surface can reach the peak earlier, and its value is higher. As shown in Figure 17, the average coalescence frequency also has a higher level in the evolution process. This results in more coalescence growth behaviors of the maximum droplet on the condensation surface and eventually promotes the contribution proportion of coalescence growth to the largest droplet size.

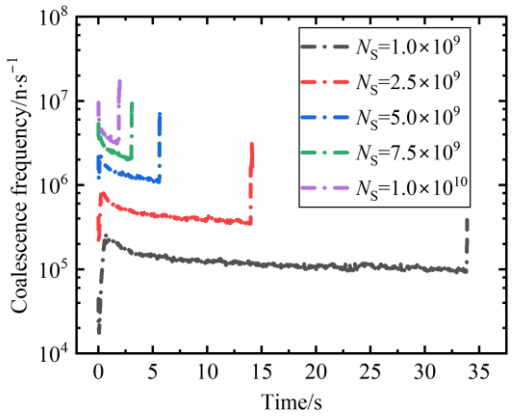

Figure 16. Comparison of coalescence frequency under different nucleus densities.

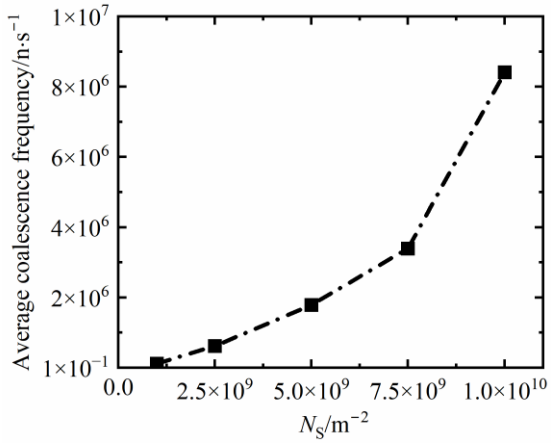

Figure 17. Average coalescence frequency under different nucleus densities.

However, the size of growth of the maximum droplet is mainly derived from the coalescence growth, so the high density of the condensation nucleus contributes to the improvement of the evolution rate and accelerates the evolution process. These verify the conclusions arrived at in Sections 3.2.1 and 3.3.2. In contrast, due to the influence of the high coalescence frequency of droplet swarm on the surface with high nucleus density, the condensation surface is rapidly occupied by relatively larger droplets. However, the condensation growth capacity of large-sized droplets is less desirable because of the influence of heat transfer, so the contribution proportion of condensation growth to the maximum droplet size is relatively weakened during the evolution process.

4. Conclusions

To sum up, based on the new model of the whole evolution process of dropwise condensation, the numerical simulation method was used to research the evolution process of dropwise condensation on the vertical hydrophobic surface. For the convenience of calculation, the simulation assumes that the droplets have the same contact angle and shape as the spherical crown, and the coalescence behavior is completed instantaneously. In addition to this, the formation position of condensation nuclei is fixed, and the condensation nuclei demonstrate uniformly random distribution.

The model consists of three parts: nucleation or renucleation model, growth model, and departure model of the droplet. This paper improves the departure model of droplets to update the spatial position and velocity of the departure droplet. The droplet renucleation model is refined and the judgment conditions of regional renucleation are added. Condensation growth and coalescence growth behavior of droplets were integrated into the model of droplet growth. The concepts of evolution rate and size contribution are proposed to study droplet growth characteristics.

Dropwise condensation in this paper refers to the process, including the initial nucleation of droplets on the surface, the condensation growth and coalescence growth of the droplet swarm, the repeated droplet renucleation, and the droplet departure in the end. As the droplet size distribution on the surface is gradually stable, the condensation heat transfer is also in a steady state. This paper compares the simulation results with experimental results and the theoretical model to verify the reliability of the simulation method and investigates the evolution process of dropwise condensation and droplet growth with different condensation nucleus densities. The conclusions are represented below:

(1) The maximum radius growth rate can better indicate the evolution rate of dropwise condensation than the average droplet size rate;
(2) The enhancement in condensation nucleus density contributes to a linear increase in the evolution rate of dropwise condensation, thereby accelerating the evolution process;
(3) At low condensation nucleus density (less than $N_S = 5 \times 10^9$ m^{-2}), with the increase of condensation nucleus density, the heat transfer capacity of the condensation surface is significantly improved. However, there is a critical value, $N_S = 5 \times 10^9$ m^{-2}. As the nucleus density exceeds such a value, the average heat flux decreases after gradually reaching its peak, $q_{average} = 30.5$ kW·m^{-2};
(4) Compared to condensation growth, coalescence growth has a more significant effect on the evolution process of dropwise condensation. More than 95% of the maximum droplet size throughout the condensation evolution process originates from coalescence growth, while the effect of condensation growth is minor;
(5) The surfaces with high coalescence frequency can augment the contribution of the coalescence growth to the maximum droplet size more effectively. Conversely, the contribution of condensation growth is weakened, which is less than 1% at the $N_S = 7.5 \times 10^9$ m^{-2}.

The above findings provide new ideas for accelerating the evolution process of dropwise condensation and enhancing heat transfer. In the industrial application of vapor condensation, we hope that the largest droplet can grow rapidly with the help of high-frequency coalescence behavior, thus expediting the evolution process of dropwise condensation and improving the cleaning period of the droplet on the surface. Eventually, it is conducive to collecting water and enhancing the heat transfer rate within a certain range.

Author Contributions: Conceptualization, Y.G.; methodology, Y.G.; software, D.Z.; validation, R.W. and D.Z.; formal analysis, R.W. and D.Z.; resources, Y.G. and L.G.; data curation, R.W.; writing—original draft, R.W.; writing—review & editing, R.W.; supervision, Y.G., L.G. and S.S.; project administration, L.G.; funding acquisition, S.S. All authors have read and agreed to the published version of the manuscript.

Funding: This research is supported by the project of National Natural Science Foundation of China (No. 52106075 & No. 51936002) and the Provincial Natural Science Foundation of Liaoning (No. 2021-MS-130). The authors are grateful for the support.

Data Availability Statement: Not applicable.

Conflicts of Interest: The authors declare no conflict of interest.

Nomenclature

a	acceleration of the droplet (m/s^2)
x	x-coordinate of the droplet
c	capillary force constant
x_i	x-coordinate of one of the adjacent droplets (m)
F_c	capillary force (N)
x_j	x-coordinate of the other of the adjacent droplets (m)

F_{g}	gravity force (N)
$x_{\min}$	x-coordinate of the condensation nucleus (m)
G	growth rate of dropwise condensation (m/s)
x_{side}	x-coordinate of the droplet closest to the condensation nucleus (m)
G/g	acceleration of gravity (m/s^2)
x_{new}	x-coordinate of new droplet formed by the coalescence (m)
H_{fg}	latent heat of condensed water ($J \cdot kg^{-1}$)
y	y-coordinate of the droplet
h_{i}	heat transfer coefficient of gas-liquid section ($W \cdot m^{-2} \cdot K^{-1}$)
y_{b}	y-coordinate of the droplet before the droplet departure within Δt(m)
k_{w}	thermal conductivity of water ($W \cdot m^{-1} \cdot K^{-1}$)
y_i	y-coordinate of one of the adjacent droplets (m)
k_{δ}	thermal conductivity of hydrophobic membrane ($W \cdot m^{-1} \cdot K^{-1}$)
y_j	y-coordinate of the other of the adjacent droplets (m)
l	mesh spacing (m)
$y_{\min}$	y-coordinate of the condensation nucleus (m)
l_{ij}	distance between adjacent droplets (m)
y_{n}	y-coordinate of the droplet after the droplet departure within Δt(m)
N_{S}	condensation nucleus density (m^{-2})
y_{new}	y-coordinate of new droplet formed by the coalescence (m)
q_{d}	droplet heat transfer rate ($kW \cdot m^{-2}$)
y_{side}	y-coordinate of the droplet closest to the condensation nucleus (m)
r	radius of the droplet (m)
z	z-coordinate of the droplet
r_b	radius of the droplet before the condensation growth within Δt(m)
z_i	z-coordinate of one of the adjacent droplets (m)
r_{c}	critical radius (m)
z_j	z-coordinate of the other of the adjacent droplets (m)
r_i	radius of one of the adjacent droplets (m)
$z_{\min}$	z-coordinate of the condensation nucleus (m)
r_j	radius of the other the adjacent droplets (m)
z_{new}	z-coordinate of new droplet formed by the coalescence (m)
$r_{\max(i,j)}$	the maximum radius of the adjacent droplets (m)
z_{side}	z-coordinate of the droplet closest to the condensation nucleus (m)
$r_{\min}$	initial nucleation radius (m)
σ	surface tension coefficient ($N \cdot m^{-1}$)
r_n	radius of the droplet after the condensation growth within (m)
ρ	density of condensate water ($kg \cdot m^{-3}$)
r_{new}	radius of new droplet formed by the coalescence (m)
δ	thickness of hydrophobic coating (m)
r_{side}	radius of the droplet closest to the condensation nucleus (m)
θ	contact angle of droplet (°)
$S_{\Delta t}$	distance of droplet departure within Δt(m)
θ_{r}	droplet regression angle (°)
T_{sat}	Saturation temperatures (K)
θ_{a}	droplet advance angle (°)
V_i	volume of one of the adjacent droplets (m^3)
Δr_h	the size contribution of coalescence growth behavior (m)
V_j	volume of the other the adjacent droplets (m^3)
Δr_l	the size contribution of condensation growth behavior (m)
V_{new}	volume of new droplet formed by the coalescence (m^3)
ΔT	surface subcooling (K)
v_b	initial velocity of the droplet (m/s)
Δt	step size (s)
v_n	the droplet detachment velocity after Δt(m/s)

References

1. Tang, G.; Hu, H. Advances in vapor dropwise condensation heat transfer. *Chin. Sci. Bull.* **2020**, *65*, 1653–1676. (In Chinese) [CrossRef]
2. Wen, F. Microscopic Mechanism of Steam Dropwise Condensation at Low Pressure and Heat Transfer Enhancement. Ph.D. Thesis, Dalian University of Technology, Dalian, China, 2014.
3. Rose, J.W. Dropwise condensation theory and experiment: A review. *Proc. Inst. Mech. Eng. Part A* **2002**, *216*, 115–128. [CrossRef]
4. Peng, Q.; Jia, L. Analysis of droplet dynamic behavior and condensation heat transfer characteristics on rectangular microgrooved surface with CuO nanostructures. *Int. J. Heat Mass Tran.* **2019**, *130*, 1096–1107. [CrossRef]
5. Suss, M.E.; Presser, V. Water desalination with energy storage electrode materials. *Joule* **2018**, *2*, 10–15. [CrossRef]
6. Wen, R.; Xu, S. Capillary-driven liquid film boiling heat transfer on hybrid mesh wicking structures. *Nano Energy* **2018**, *51*, 373–382. [CrossRef]
7. Stark, A.K.; Klausner, J.F. An R&D strategy to decouple energy from water. *Joule* **2017**, *1*, 416–420. [CrossRef]
8. Schmidt, E.; Schurig, W. Condensation of water vapour in film-and drop form. *Tech. Mech. Thermodyn.* **1930**, *1*, 53–63.
9. Graham, C.; Griffith, P. Drop size distributions and heat transfer in dropwise condensation. *Int. J. Heat Mass Tran.* **1973**, *16*, 337–346. [CrossRef]
10. Gose, E.E.; Mucciardi, A.N. Model for dropwise condensation on randomly distributed sites. *Int. J. Heat Mass Tran.* **1967**, *10*, 15–22. [CrossRef]
11. Rose, J.W.; Glicksman, L.R. Dropwise condensation—The distribution of drop sizes. *Int. J. Heat Mass Tran.* **1973**, *16*, 411–425. [CrossRef]
12. Tanasawa, I. Dropwise condensation the way to practical applications. In Proceedings of the International Heat Transfer Conference Digital Library, Toronto, ON, Canada, 7–11 August 1978. [CrossRef]
13. Chen, J.C. Surface contact—Its significance for multiphase heat transfer: Diverse examples. *J. Heat Transfer.* **2003**, *125*, 549–566. [CrossRef]
14. Peng, B.; Ma, X. Experimental investigation on steam condensation heat transfer enhancement with vertically patterned hydrophobic–hydrophilic hybrid surfaces. *Int. J. Heat Mass Tran.* **2015**, *83*, 27–38. [CrossRef]
15. Chen, X.; Derby, M.M. Combined visualization and heat transfer measurements for steam flow condensation in hydrophilic and hydrophobic mini-gaps. *J. Heat Transfer.* **2016**, *138*, 091503. [CrossRef]
16. Alwazzan, M.; Egab, K. Condensation on hybrid-patterned copper tubes (I): Characterization of condensation heat transfer. *Int. J. Heat Mass Tran.* **2017**, *112*, 991–1004. [CrossRef]
17. Bhattarai, B.; Priezjev, N.V. Wetting properties of structured interfaces composed of surface-attached spherical nanoparticles. *Comput. Mater. Sci.* **2018**, *143*, 497–504. [CrossRef]
18. Ashrafi-Habibabadi, A.; Moosavi, A. Droplet condensation and jumping on structured superhydrophobic surfaces. *Int. J. Heat Mass Tran.* **2019**, *134*, 680–693. [CrossRef]
19. Aili, A.; Ge, Q. How nanostructures affect water droplet nucleation on superhydrophobic surfaces. *J. Heat Transfer.* **2017**, *139*, 112401. [CrossRef]
20. Lefevre, E.J.; Rose, J.W. A theory of heat transfer by dropwise condensation. In Proceedings of the International Heat Transfer Conference Digital Library, Chicago, IL, USA, 7–12 August 1966. [CrossRef]
21. Maa, J.R. Drop size distribution and heat flux of dropwise condensation. *Chem. Eng. J.* **1978**, *16*, 171–176. [CrossRef]
22. Miljkovic, N.; Enright, R. Modeling and optimization of superhydrophobic condensation. *J. Heat Transfer.* **2013**, *135*, 111004. [CrossRef]
23. Liu, X.; Cheng, P. Dropwise condensation theory revisited: Part I. Droplet nucleation radius. *Int. J. Heat Mass Tran.* **2015**, *83*, 833–841. [CrossRef]
24. Han, X.; Han, Z. Coupled model of heat and mass balance for droplet growth in wet steam non-equilibrium homogeneous condensation flow. *Energies* **2017**, *10*, 2033. [CrossRef]
25. Shang, Y.; Hou, Y. Modeling and optimization of condensation heat transfer at biphilic interface. *Int. J. Heat Mass Tran.* **2018**, *122*, 117–127. [CrossRef]
26. Xie, J.; Xu, J. Dropwise condensation on superhydrophobic nanostructure surface, part II: Mathematical model. *Int. J. Heat Mass Tran.* **2018**, *127*, 1170–1187. [CrossRef]
27. Burnside, B.M.; Hadi, H.A. Digital computer simulation of dropwise condensation from equilibrium droplet to detectable size. *Int. J. Heat Mass Tran.* **1999**, *42*, 3137–3146. [CrossRef]
28. Liu, X.; Cheng, P. Lattice Boltzmann simulation for dropwise condensation of vapor along vertical hydrophobic flat plates. *Int. J. Heat Mass Tran.* **2013**, *64*, 1041–1052. [CrossRef]
29. Pawar, N.D.; Kondaraju, S. Effect of Surface Wettability on Dropwise Condensation Using Lattice Boltzmann Method. In Proceedings of the International Conference on Micro/Nanoscale Heat Transfer, Singapore, 3–6 January 2016. [CrossRef]
30. Bahrami, H.R.T.; Saffari, H. Theoretical study of stable dropwise condensation on an inclined micro/nano-structured tube. *Int. J. Refrig.* **2017**, *75*, 141–154. [CrossRef]
31. Zhao, C.; Yan, X. Numerical simulation of droplet size distribution in the whole process of droplet condensation. *J. Eng.* **2020**, *41*, 1485–1490. (In Chinese)

32. Azarifar, M.; Budakli, M. On the individual droplet growth modeling and heat transfer analysis in dropwise condensation. *IEEE Trans. Compon. Packag. Manuf. Technol.* **2021**, *11*, 1668–1678. [CrossRef]
33. Sun, J.; Wang, H.S. On the early and developed stages of surface condensation: Competition mechanism between interfacial and condensate bulk thermal resistances. *Sci. Rep.* **2016**, *6*, 35003. [CrossRef] [PubMed]
34. Niu, D.; Guo, L. Dropwise condensation heat transfer model considering the liquid-solid interfacial thermal resistance. *Int. J. Heat Mass Tran.* **2017**, *112*, 333–342. [CrossRef]
35. Rashidi, M.M.; Ghahremanian, S. Effect of solid surface structure on the condensation flow of Argon in rough nanochannels with different roughness geometries using molecular dynamics simulation. *Int. Commun. Heat Mass Transfer.* **2020**, *117*, 104741. [CrossRef]
36. Ghahremanian, S.; Abbassi, A. Investigation the nanofluid flow through a nanochannel to study the effect of nanoparticles on the condensation phenomena. *J. Mol. Liq.* **2020**, *311*, 113310. [CrossRef]
37. Hekmatifar, M.; Toghraie, D. Molecular dynamics simulation of condensation phenomenon of nanofluid on different roughness surfaces in the presence of hydrophilic and hydrophobic structures. *J. Mol. Liq.* **2021**, *334*, 116036. [CrossRef]
38. Cui, H.; Saleem, S. Effects of roughness and radius of nanoparticles on the condensation of nanofluid structures with molecular dynamics simulation: Statistical approach. *J. Taiwan Inst. Chem. Eng.* **2021**, *128*, 346–353. [CrossRef]
39. Ghahremanian, S.; Abbassi, A. Molecular dynamics simulation of annular condensation of vapor argon through a nanochannel for different saturation conditions with focusing on the flow and heat transfer. *Int. Commun. Heat Mass Transfer.* **2020**, *116*, 104704. [CrossRef]
40. Tammann, G.; Boehme, W. Die Zahl der Wassertröpfchen bei der Kondensation auf verschiedenen festen Stoffen. *Ann Phys-Berlin.* **1935**, *414*, 77–80. [CrossRef]
41. Khandekar, S.; Muralidhar, K. *Dropwise Condensation on Inclined Textured Surfaces*; Springer: New York, NY, USA, 2014; pp. 45–75. [CrossRef]
42. Abu-Orabi, M. Modeling of heat transfer in dropwise condensation. *Int. J. Heat Mass Tran.* **1998**, *41*, 81–87. [CrossRef]
43. Kim, S.; Kim, K.J. Dropwise condensation modeling suitable for superhydrophobic surfaces. *ASME J. Heat Transfer.* **2011**, *133*, 081502. [CrossRef]
44. Xu, W.; Lan, Z. Droplet size distributions in dropwise condensation heat transfer: Consideration of droplet overlapping and multiple re-nucleation. *Int. J. Heat Mass Tran.* **2018**, *127*, 44–54. [CrossRef]
45. Xu, Z.; Zhang, L. Multiscale dynamic growth and energy transport of droplets during condensation. *Langmuir* **2018**, *34*, 9085–9095. [CrossRef]
46. Ristenpart, W.D.; McCalla, P.M. Coalescence of spreading droplets on a wettable substrate. *Phys. Rev. Lett.* **2006**, *97*, 064501. [CrossRef] [PubMed]
47. Wen, R.; Lan, Z. Droplet dynamics and heat transfer for dropwise condensation at lower and ultra-lower pressure. *Appl. Therm. Eng.* **2015**, *88*, 265–273. [CrossRef]

Disclaimer/Publisher's Note: The statements, opinions and data contained in all publications are solely those of the individual author(s) and contributor(s) and not of MDPI and/or the editor(s). MDPI and/or the editor(s) disclaim responsibility for any injury to people or property resulting from any ideas, methods, instructions or products referred to in the content.